Effect of dopant concentration and particle size on fluorescence properties of Y$_2$O$_3$:Eu^{3+} derived in presence of NIPAM/AAc copolymer

Shahrzad Fadaie · Mohammad Mehdi Kashani-Motlagh · Amir Maghsoudipour · Bita Faridnia

Abstract Y$_2$O$_3$:Eu^{3+} nano phosphors (about 65 nm in size) were prepared via co-precipitation method by using co-polymer NIPAM/AAc as a template with narrow size distribution. The aim of the paper is to indicate the co-polymer influence on size and luminescence characteristics of nano phosphors. In this respect, phase content and morphology were characterized by X-ray diffraction and transmission electron microscopy. All the powders were well crystallized and the particles were clearly spherical with good dispersibility. Luminescence measurements were used to investigate the role of precursor in powders and the utmost luminescence intensity was observed at 4 mol% of Eu^{3+} while the quenching concentration of Eu^{3+} ions has occurred at 5 mol%.

1 Introduction

Yttrium oxide is a suitable host for many lanthanide oxides because of the resemblance between their ionic radius and crystal structure and doping most of these oxides produce variety of phosphors with different fluorescent spectra i.e. green for Tb, red for Eu, Yellow for Dy, blue for Tm [1, 2]. Among these phosphors, Y$_2$O$_3$:Eu^{3+} is well-known red phosphor typically used in field emission display (FED) devices, cathode ray tubes (CRT) applications, trichromatic fluorescent lamps and plasma display panels [3–7]. The fluorescence property of Y$_2$O$_3$:Eu^{3+} strongly depends on its structure. Commercial type of this phosphor has the cubic structure because the cubic structure with space group: Ia3 (206) possesses great potential of fluorescence intensity compare to the monoclinic structure with space group of C2/m(12) [8–10]. The cubic lattice contains two crystallographic sites in which the M^{3+} ions are found as outlined in Fig. 1, one has C$_2$ symmetry and the other S$_6$ symmetry; both sites are six coordinate and are present the ratio of 3:1 [11–13]. In particular, europium (III) has five narrow emission bands corresponding to the $^5D_0 \rightarrow {}^7F_i$ transitions where i = 0, 1, 2, 3 and 4. The strongest transition, $^5D_0 \rightarrow {}^7F_2$ occurs at approximately 610 nm, which is characteristic of red fluorescence of Eu^{3+} [14].

Some qualities including high purity level of host structure, doping concentration of Eu and particle size have the most important influences on industrial fabrication of nanophosphor Y$_2$O$_3$:Eu^{3+}. In order to produce a nanophosphor with high quality, a variety of synthesis methods has been studied such as: sol–gel [3], spray pyrolysis [9], hydrothermal decomposition [15], chemical precipitation of precursors in aqueous or organic solutions and addition of modifying agents such as: EDTA and polymers as a template [16–19]. In the present work, mono-dispersed nanophosphor Y$_2$O$_3$:Eu^{3+} particles are synthesized in urea aqueous solution by homogeneous precipitation method. The effect of experimental variables, such as: presence of NIPAM/AAc co-polymer as a template, size distribution and europium concentrations were characterized in terms of luminescence properties.

2 Experimental procedures

2.1 Starting materials

The entire chemical materials which are used in this work were obtained from Merck Fine Chemicals.

S. Fadaie (✉) · M. M. Kashani-Motlagh · B. Faridnia
Chemistry Department, Iran University of Science
and Technology, 6 No. 9 Banafsheh St. Etaati jonoubi Av.
Marzdaran Blvd., 1464734643 Tehran, Iran
e-mail: sh_fadaie2002@yahoo.com

A. Maghsoudipour
Ceramic Department, Materials and Energy Research Centre,
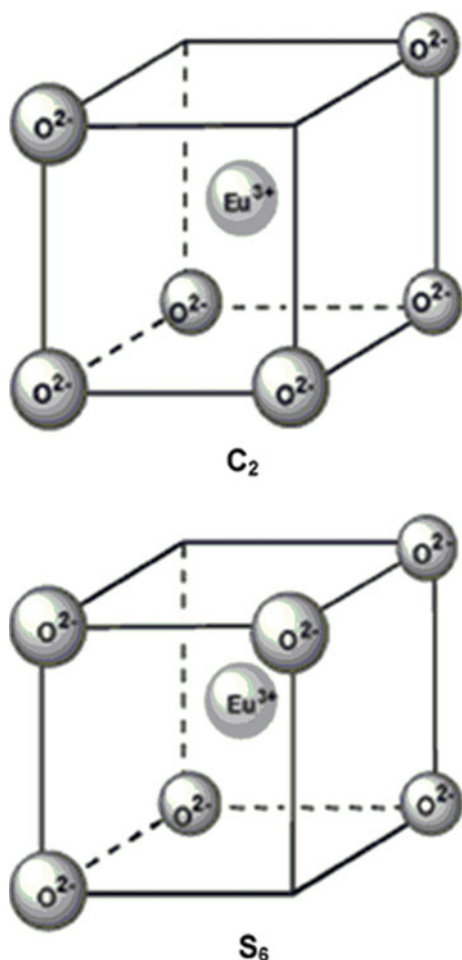Tehran, Iran

Fig. 1 Two Y^{3+} crystallographic sites in cubic Y_2O_3

2.2 Synthesis of europium doped yttria

Y_2O_3:Eu^{3+} was prepared via homogeneous precipitation method by utilizing NIPAM/AAc as a template and urea as a precipitant while the preparation of the copolymer is described perfectly in our previous study [20]. In order to prepare Y_2O_3 phase with the copolymer a known amount of $Y(NO_3)_3$

$$\frac{56.4g}{l}$$

and $Eu(NO_3)_3$ (2–8 mol% with respect to Y) were prepared by dissolving Eu_2O_3 and Y_2O_3 in dilute HNO_3. Then, an excess amount of urea is dissolved in the vessel and mixed with the above solutions thoroughly. Then 30 ml of NI-PAM/AAc copolymer was added to the solution at adjusted pH of 3 to complete the precipitation reaction and the temperature is raised up to 85 °C for 1 h. The resulting precipitates were separated and washed with ethanol and to dry the precipitates, it was put into oven and pre-heated at 100 °C overnight. Finally, calcinations treatment was carried out in a muffle furnace for 3 h at 980 °C. Also to

compare the physico-chemical effects of the copolymer, a sample without copolymer was prepared and the precursor solutions containing $Y(NO_3)_3$ and Eu_2O_3 (2 wt%) in dilute HNO_3 were used.

2.3 Physical measurements

The crystal structure of the Y_2O_3 phase was identified by X-ray diffraction (XRD, Siemens D-500; Cu$k\alpha$ radiation at 40 kV and 30 mA). The particle size and distribution of prepared samples were analyzed using a Malvern Zeta Sizer after the preparation. The samples had to be diluted in water and they were also inserted in an ultrasonic bath for 10 min. Microstructure of the samples was observed by scanning electron microscope (SEM) Cambridge at a voltage of 25 kV sputtered by gold. The emission and excitation spectra were obtained using a Perkin Elmer LS-5 Luminescence spectroscopy.

3 Result and discussion

3.1 X-ray powder diffraction analysis

X-ray diffraction (XRD) patterns of Y_2O_3/Eu^{3+} prepared at 980 °C is shown in Fig. 2. As it is clear, there is no evidence of appearing two assigned peaks of monoclinic phase at $2\theta = 32.1°$ and $29.78°$ and all the peaks are in good agreement with powder data in JCPDS card No. 25-1011. According to that, the samples are cubic crystalline Y_2O_3:Eu^{3+} without impurity [21]. In addition, comparing XRD patterns of samples (a and b) shows that cubic phase of Y_2O_3 is formed completely and both samples have the similar crystallinity regardless of NIPAM/AAc copolymer. Also, it could indicate that the doped Eu^{3+} ions have entered the Y^{3+} sites completely because usually, doping into space among crystal lattice will cause lattice distortion and then origin the change of the cell parameters.
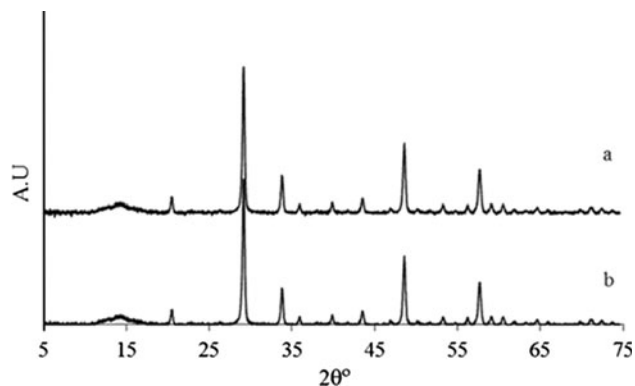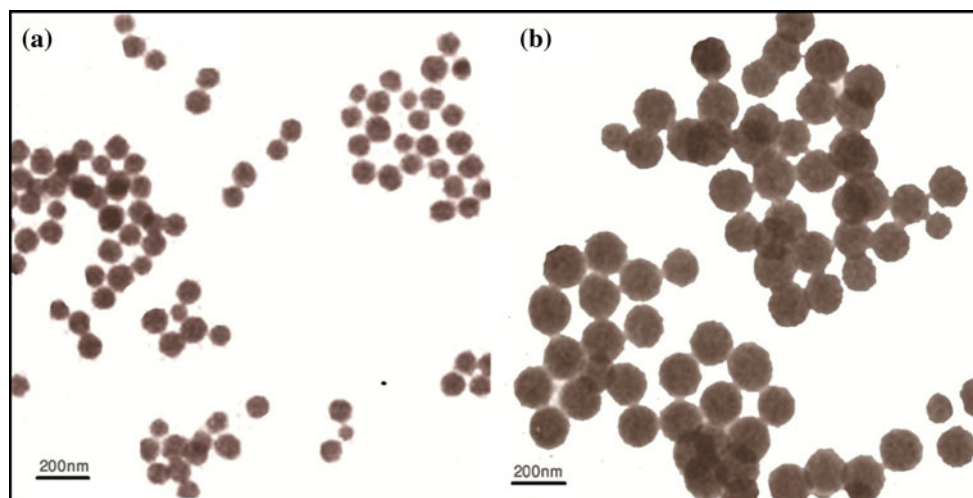

Fig. 2 XRD patterns of Y_2O_3/Eu^{3+} prepared (*a*) with, (*b*) without copolymer

Fig. 3 TEM micrograph of nonoparticles $Y_2O_3:Eu^{3+}$prepared (*a*) with, (*b*) without copolymer

3.2 Luminescent analysis

3.2.1 Particle size effect on emission spectra

The proposed mechanism for the formation of the phosphor precursor of $Y_2O_3:Eu^{3+}$ explains the cause of decreasing the particle size in presence of NIPAM/AAc co-polymer [22, 23]. The carboxyl groups incorporated into the molecule of the copolymer by adding the AAc; give it a negative surface charge. On the other hand, decomposition of urea increases pH and the hydrolyzed yttrium ions by water will combine with anionic groups on the surface of the copolymer micro-gel, meantime hydroxyl carbonate precursor forms and links to the copolymer. The final particle is a copolymer coated by the hydroxyl carbonate precursor of the phosphor. After annealing treatment the copolymer decomposed and the final $Y_2O_3:Eu^{3+}$ nanophosphor formed. Thus the particle of the sintered phosphor is more regular and the size is small due to the presence of the copolymer. The TEM micro-graphs (Fig. 3a, b) show the particles morphology of the obtained $Y_2O_3:Eu^{3+}$ nanoparticles with/without copolymer precursor, respectively. It can be seen that both samples have a non-agglomerated spherical shape with clear particle boundaries and were nano-sized. Fig. 4a, b illustrate mean particle size of 65 and 170 nm for both samples. It is clear that the sample with co-polymer contains particles portion with diameters from 55 to 65 nm while the sample without the copolymer (Fig. 4b) owns the particles portion with diameters from about 165 to 173 nm. It is obvious that NIPAM/ACC co-polymer has influence on the growth sur-roundings of the particle and the variation of particle sizes is a direct function of that [24]. This co-polymer can prevent the agglomeration of nanoparticles by reducing the surface tension and also prevents particles from contacting with each other by steric-hindrance effect. So, the particles diameter can be restricted to less than 65 nm.

As shown in Fig. 5 the emissions spectrum patterns under 254 nm excitation for the prepared samples with/without copolymer were analogous to each other and there is no position change of the emission peaks for both powders, but the intensity is appeared to be dissimilar according to two different type of synthesis media. The spectra are composed of notable peaks at 582, 587, 592, 598 and 610 nm. The transitions ranging from 582 to 598 nm are assigned to the site selection of europium in host matrix and occupancy of the symmetric S6 site by the Eu^{3+} ion [25–30], while the strongest one at 610 nm is attributed to $^5D_0 \rightarrow {}^7F_2$ transition in the C_2 site of Y_2O_3 [27, 31]. It was reported that among two Y^{3+} sites in cubic Y_2O_3; 75 % of these have C_2 symmetry and 25 % are sites with S_6 inversion symmetry [13, 32]. The emission spectra clearly shows that precipitation process with the NIPAM/AAc co-polymer alike traditional synthesis method, leads the europium cations to occupy C_2 sites too. Furthermore, synthesised sample has higher intensity than sample with-out co-polymer, because Eu^{3+} ions enter the Y_2O_3 crystal
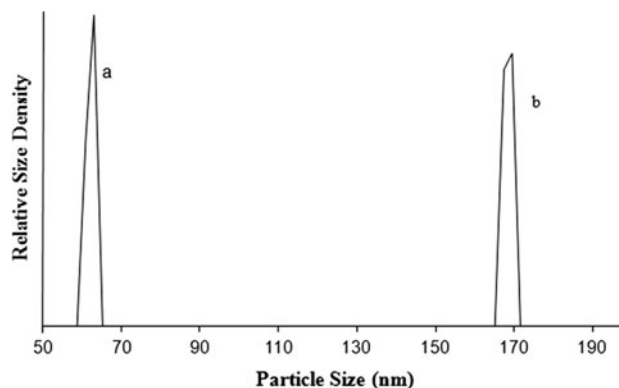

Fig. 4 Size distribution diagram of nanoparticles $Y_2O_3:Eu^{3+}$ pre-pared (*a*) with, (*b*) without copolymer
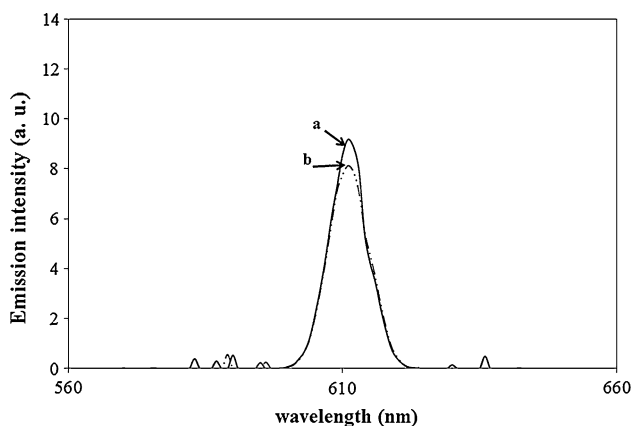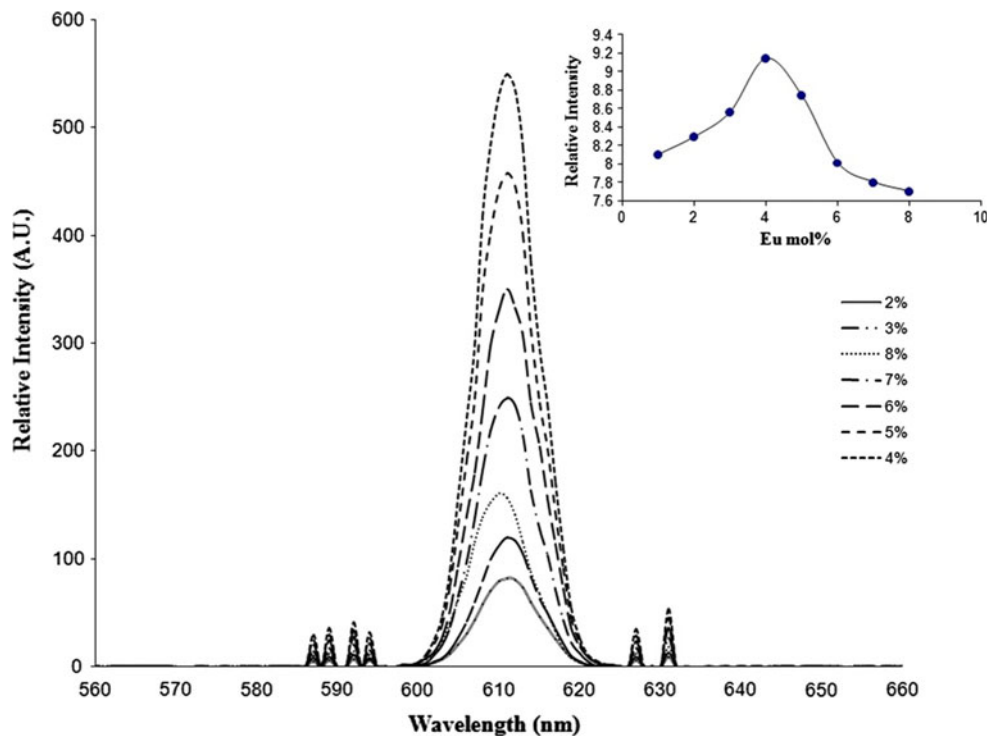
Fig. 5 Emission spectra of the nanophosphors Y_2O_3:Eu^{3+} prepared (*a*) with, (*b*) without copolymer

lattice more easily in the presence of NIPAM/AAc co-polymer due to decrease of particle size. Thus, the activator concentration is higher although the same amount of Eu^{3+} is doped in the Y_2O_3 host in both methods.

3.2.2 Europium concentration effect on emission spectra

In order to determine the effect of the Eu^{3+} concentration on luminescence intensity, different concentrations (Eu^{3+}/Y^{3+} mol ratio: 0.02, 0.03, 0.04, 0.05, 0.06, 0.07 and 0.08) of Eu^{3+} doped Y_2O_3 nanoparticles were synthesized via NIPAM/AAc co-polymer route. The emission intensity of Y_2O_3:Eu^{3+} with respect to the doping concentration of the Eu ions is

shown in Fig. 6. Initially, the emission intensity increased with increasing Eu/Y up to Eu/Y = 0.04 mol ratio, and then started reducing with increasing Eu^{3+} concentration which is due to critical quenching concentration of Eu^{3+}. The critical quenching concentration is defined as the concentration at which the emission intensity begins to decrease during the increase of Eu^{3+} concentration [33]. The quenching effect occurs since the interaction between activator ions increases [34]. As stated in Sect. 3.2.1, there is an excellent probability of entering Eu^{3+} in both sites of S_6 and C_2 which generates strong interaction among activator sites. It means, by increasing Eu^{3+} concentration from 0.02 to 0.08 mol and enhancing the number of activator centers, the emission from one Eu center will be quenched by transferring excitation energy to another Eu center. This transformation between the centers would proceed till the excitation energy quenches, so the luminescence intensity would decrease. Thus, the critical quenching concentration of Eu^{3+} in prepared Y_2O_3:Eu^{3+} with co-polymer nanophosphor is 0.05 mol.

4 Conclusions

In conclusion, Y_2O_3:Eu^{3+} nano phosphor is prepared via a precipitation method using a NIPAM/AAc co-polymer successfully. This process proves to be very useful, simple and whilst pure cubic Y_2O_3:Eu^{3+} nano-powder with high homogeneity can be obtained. The results reveal that NIPAM/AAc copolymer has remarkably diminished the

Fig. 6 Emission spectra of samples prepared with copolymer in different Eu^{3+} concentration. The *inset* shows the effect of Eu mol% on the emission intensity. All samples were excited using a wavelength of 254 nm

particle size from 165 to 65 nm while all the particles shaped clearly spherical and non-agglomerated. In comparison with the phosphors prepared by a conventional method, the emission intensity of Y_2O_3:Eu^{3+} nanopowder revealed that the nature of co-polymer influences the luminescence characteristics of nano phosphors and doping Eu^{3+} ions at a suitable content (4 mol%) can greatly improve the luminescence intensity. In contrast, emission intensity reduced in the case of increasing Eu^{3+} concentration and the quenching effect was observed at the concentration 5 mol% of Eu^{3+}. All the results indicate that Y_2O_3:Eu^{3+} nanopowder prepared by using co-polymer NIPAM/AAc template is a promising red phosphor with high luminescence intensity.

References

1. J. Hao, S.A. Studenikin, M. Cocivera, J. Lumin. **93**, 313 (2001). doi:10.1016/S0022-2313(01)00207-1
2. F. Vetrone, J.C. Boyer, J.A. Capobianco, A. Speghini, M. Bettinelli, Nanotechonology **15**, 75 (2004). doi:10.1088/0957-4484/15/1/015
3. P.K. Sharma, M.H. Jilavi, V.K. Varadan, H. Shmidt, J. Phys. Chem. Solid **63**, 171 (2002). doi:10.1016/S0022-3697(01)00124-X
4. N. Joffin, J. Dexpert-Ghys, M. Verelst, G. Baret, A. Garcia, J. Lumin. **113**, 249 (2005). doi:10.1016/j.jlumin.2004.10.021
5. K. Pramod, P.K. Sharma, R. Nass, H. Schmidt, Opt. Mater. **10**, 169 (1998). doi:10.1016/S0925-3467(97)00140-7
6. Y. Qi, L. Sun, M. Lee, B.I. Samuels, G.J. Exarhos, J. Lumin. **109**, 85 (2004). doi:10.1016/j.jlumin.2004.01.085
7. B. Guoa, H. Yima, W. Hwanga, M. Nowellb, Z. Luoc, Particuology **9**, 24 (2011). doi:10.1016/j.partic.2010.07.020
8. X. Qin, Y.G. Ju, S. Bernhard, N. Yao, J. Mater. Res. **20**, 2960 (2005). doi:10.1557/JMR.2005.0364
9. D. Dosev, B. Guo, I.M. Kennedy, J. Aerosol Sci. **37**, 402 (2006)
10. A. Camenzind, R. Strobel, F. Krumeich, S.E. Pratsinis, Adv. Powder Technol. **18**, 5 (2007). doi:10.1163/156855207779768142
11. M.G. Paton, E.N. Maslem, Acta. crystallogr. **19**, 307 (1965). doi:10.1107/S0365110X65003365
12. H. Ishibashi, K. Shimomoto, K. Nakahigashi, J. Phys. Chem. Solids **55**, 809 (1994). doi:10.1021/jp0102522
13. M. Mitric, B. Antic, M. Balanda, D. Rodic, M.L. Napijalo, J. Phys. Condens. Matter **9**, 4103 (1997)
14. B.C. Joshi, J. Non-Cryst. Solids **180**, 217 (1995). doi:10.1016/0022-3093(94)00478-1
15. X.B. Hong, L. Yu, L. Yang, Z. Liu, G. Pan, S. Lu, X. Ren, Y. Lei, L. Fan, J. Phys. Chem. B **109**, 15236 (2005). doi:10.1016/S1466-6049(00)00065-9
16. P.K. Sharma, M.H. Jilavi, H. Schmidt, V.K. Varadan, Int. J. Inorg. Matter **2**, 407 (2000). doi:10.1016/S1466-6049(00)00065-9
17. X. Jing, T. Ireland, C. Gibbons, D.J. Barber, J. Silver, A. Vecht, G. Fern, P. Trowga, D.C. Morton, J. Electrochem. Soc. **146**, 4654 (1999)
18. M.I. Martinez-Rubio, T.J. Ireland, J. Silver, G. Fern, C. Gibbons, A. Vecht, Electrochem. Solid-State Lett. **3**, 446 (2000). doi:10.1002/chin.200049231
19. Z. Yongqing, Y. Zihua, D. Shiwen, Q. Mande, Z Jian Mater. Lett. **57**, 2901 (2003). doi:10.1016/S0167-577X(02)01394-0
20. Sh Fadaie, M.M. Kashani-Motlagh, A. Maghsoudipour, B. Faridnia, Pigment Resin Technol. **39**, 214 (2010). doi:10.1108/03699421011055527
21. S. Katagiri, N. Ishizawa, F. Marumo, Powder Diffr. **8**, 60 (1993)
22. J. Silver, M.I. Martinez-Rubio, S. Gebretensae, G.R. Fern, M.J. Snowden, R. Withnall, SID Symp. Dig. Tech. Pap. **33**, 393 (2002)
23. S. Zhong, J. Chen, S. Wang, Q. Liu, Y. Wang, S. Wang, J. Alloy. Compd. **493**, 322 (2010). doi:10.1016/j.jallcom.2009.12.092
24. X.H. Liu, J. Yang, L. Wang, X.J. Yang, L.D. Lu, X. Wang, Mater. Sci. Eng. A **289**, 241 (2000). doi:10.1016/S0921-5093(00)00901-1
25. F. Parasapour, D.F. Kelley, R.S. Williams, J. Phys. Chem. B **102**, 7971 (1998). doi:10.1021/jp982628q
26. D.B.M. Klaassen, R.A.M. Van Ham, T.G.M. Van Rijn, J. Lumin. **40**, 651 (1989). doi:10.1016/0022-2313(89)90096-3
27. M. Buijs, A. Meijerink, G. Blasse, J. Lumin. **37**, 9 (1987). doi:10.1016/0022-2313(87)90177-3
28. A. Garcia-Murillo, C.L. Luyer, C. Garapon, C. Dujardin, E. Bernstein, C. Pedrini, J. Mugnier, Opt. Mater. **19**, 161 (2002). doi:10.1016/S0925-3467(01)00214-2
29. R.E. Ouenzerfi, C. Goutaudier, M. Cohen-Adad, Th Panczer, G. Boulon, J. Lumin. **102**, 426 (2003). doi:10.1016/S0022-2313(02)00580-X
30. V. Jubera, J.P. Chaminade, A. Garcia, F. Guillen, C. Fouassier, J. Lumin. **101**, 1 (2003). doi:10.1016/S0022-2313(02)00335-6
31. R.B. Hunt, R.G. Pappalardo, J. Lumin. **34**, 3133 (1985). doi:10.1016/0022-2313(85)90085-7
32. J. Silver, M.I. Martinez-Rubio, T.G. Ireland, R. Withnall, J. Phys. Chem. B **105**, 7200 (2001). doi:10.1021/jp0102522
33. D. Wang, Q. Yin, Y. Li, M. Wang, J. Lumin. **97**, 1 (2002). doi:10.1016/S0022-2313(01)00413-6
34. Shigeo SM (1990) Phosphor Handbook, Vol **99**, CRC Press, New York, pp 108–109